Towards unblinding the surgeons: Complex electrical impedance for electrode array insertion guidance in cochlear implantation

NAUMAN HAFEEZ[1,*], XINLI DU[1], NIKOLAOS BOULGOURIS[1], PHILIP BEGG[2], RICHARD IRVING[2], CHRIS COULSAN[2] AND GUILLAUME TOURRELS[3]

[1] *Institute of Environment, Health and Societies, Brunel University, London, UK*

[2] *University Hospitals Birmingham NHS Foundation Trust, Birmingham, UK*

[3] *Oticon Medical Neurelec Inc., Vallauris, France*

The complications during electrode array insertion in scala tympani for cochlear implantation may cause trauma, residual hearing loss and affect speech outcomes. The inner ear is like a black box for surgeons during the insertion process with no real-time feedback and must rely on radiation-based extraoperative imaging. Impedance measurement of electrodes during insertion is a simple yet effective method to assess array position. For this, an impedance meter has been designed which can measure magnitude ($|Z|$), phase (θ), real (R) and imaginary (X_c) parts of impedance. A switching circuit can sequentially scan all electrode pairs at regular intervals during insertion. An Evo® straight electrode array is inserted in a transparent 2:1 scaled up 2D cochlear model (11 trials) filled with 0.9% saline using a 3-degrees-of-freedom actuation system. Bipolar impedance measurements of 8 pairs (40 samples each) are taken at regular intervals during 25 mm insertion at speed of 0.05mm/sec. A notable increase in $|Z|$ and R is observed in the apical 3 electrode pairs when they first get in to contact with the lateral wall. At the same time, the phase gets less negative (more resistive impedance) and X_c increases (less capacitance). These results show that impedance can be used for electrode array localization in cochlea and impedance change due to electrode proximity to different materials can have application in other electrode implants.

INTRODUCTION

A cochlear implant (CI) is an electronic device that provides restoration of auditory perception in patients with sensorineural hearing loss (Eshraghi *et al.*, 2012). The CI mechanism directly stimulates the nerve system by electric means bypassing the damaged sensory hair cells which are responsible for the transconduction of acoustic signals into electrical signals in a normal human ear. An electrode array (EA) inserted into scala tympani (ST) membrane of the inner ear is responsible for stimulating the nerve fibre. There are three objectives of EA insertion for better hearing outcomes:

*Corresponding author: nauman.hafeez@brunel.ac.uk

Proceedings of the International Symposium on Auditory and Audiological Research (Proc. ISAAR), Vol. 7: Auditory Learning in Biological and Artificial Systems, August 2019, Nyborg, Denmark. Edited by A. Kressner, J. Regev, J. C.-Dalsgaard, L. Tranebjærg, S. Santurette, and T. Dau. The Danavox Jubilee Foundation, 2019. ISSN: 2596-5522.

(1) deep insertion into cochlear to cover lower frequency range, (2) close proximity to the modiolus wall to ensure greater operating efficiency and (3) to preserve residual hearing by preserving inner ear structure (Rebscher *et al.*, 2008). There is always a high chance of insertion trauma to accomplish the first two goals. This includes injury to the lateral or modiolar wall and distortion of the basilar membrane which may result in loss of residual hearing, poor speech outcomes and limited device performance (Roland and Wright, 2006). Insertion failure such as tip fold over and buckling of electrode array can also have severe effects. With the advent of electro-acoustic cochlear implants and relaxation of eligibility criteria for implantation, it is even more important to save residual hearing.

The reason for these mishaps is the unavailability of real-time intraoperative feedback systems for surgeons during EA insertion. The surgery often only involves preoperative planning and postoperative evaluation using CT scan images. There is also a method to get intraoperative information through fluoroscopy but it involves radiation and its exposure could be harmful to the patient's health. There is, therefore, no safe, inexpensive and intraoperative procedure available to point out trauma or faulty array placement during surgery.

Recent advances in EA design and surgical procedure and tooling were made to keep intra-cochlear trauma to be minimum during implantation (Dhanasingh and Jolly, 2017). EA with softer material, pre-curved perimodiolar arrays, and Advance Off Stylet insertion technique are some examples. Trauma prevention, ease in insertion, better visualisation and human ear anatomy are major factors to choose insertion through the round window or cochleostomy (Richard *et al.*, 2012). These techniques have helped to relatively reduce the risk of trauma, however, failed to completely avoid it and poses other complications, for example, frequent tip folder-over during pre-curved EAs.

A magnetically guided system was presented by Clark *et al.* (2012) in which a magnetically tipped electrode array is guided by a manipulator magnet placed near the patient's head which applies magnetic torque to the tip causing it to bend away from the ST walls. One of the primary focus to avoid trauma is by reducing the insertion forces during insertion. It has been shown in studies that robotic insertion can help control insertion forces by varying insertion speed (Zhang *et al.* (2010); Kontorinis *et al.* (2011); Zhang *et al.* (2009); Rau *et al.* (2010)). These systems may reduce trauma, however, they need local position information of EA in cochlea during insertion.

6The impedance of electrodes during insertion is another feature that could be useful for array localization. Impedance magnitude measurement mechanism is built into all commercially available cochlear implants, however, it is only employed postoperatively to check the correct functioning of each electrode. Tan *et al.* (2013) and Pile *et al.* (2017) conducted experiments to observe the change in impedance magnitude before and after stylet removal of a perimodiolar electrode array

during insertion. According to their results, an increase in impedance magnitude was observed when EA comes closer to the modiolar wall after stylet removal. Giardina *et al.* (2018) looked into the relationship between the monopolar impedance magnitude of electrodes with insertion depth and proximity to the cochlear wall. The change in component values of the equivalent impedance model namely access resistance (R_a), polarization resistance (R_p) and polarization capacitance (C_p) had also been observed during insertion.

Impedance phase has not been looked into in the above studies. The objective of this study is to design an impedance meter that is able to measure bipolar impedance magnitude as well as phase. From these two measures, it is also possible to calculate the real and imaginary parts of the impedance. The proposition is that these properties would change when the electrodes interact with the walls due to disturbances in electrochemical reactions on electrode-electrolyte interface.

METHODOLOGY

Electrode Array and Cochlear Model

Oticon Medical's soft straight EVO® electrode array was used. It is a long (Insertion Length: 25 mm, Active Length: 24 mm), thin (proximal diameter = 0.5 mm; distal diameter = 0.4 mm), flexible array with a smooth silicone surface carrying 20 micro-machined titanium-iridium electrodes as shown in Fig. 1. Each electrode length is 0.47 mm and the gap between two consecutive electrodes is 0.73 mm. Electrodes are numbered from E1 to E20 where former is the basal and latter is the apical electrode. A 2:1 scaled-up plastic 2D cohlear model was used which was filled with the saline solution of 0.9% concentration as an alternative to perilymph fluid.

Actuation System and Impedance Meter

The actuation system used has two translational stages (vertical and horizontal movements) and a rotational stage and is controlled by a custom MATLAB® GUI based application. The insertion speed of the linear actuators and the insertion angle of the rotational stage can be controlled. Physik Instrumente (PI) M-404 and M-061 devices were used for translational and rotational stages respectively and PI's C-863 servo controller was used as a driver of these stages.

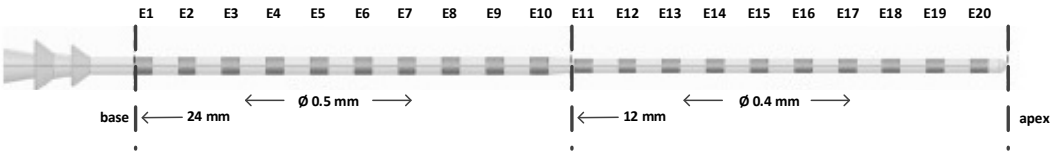

Fig. 1: Evo® Electrode Array with 20 electrodes E1-E20 (www.oticonmedical.com).

The impedance meter was designed using National Instrument's (NI) Data Acquisition

(DAQ) 6211 device having 8 differential I/O channels (or 16 single-ended), 16 bits of ADC resolution and single-channel maximum sampling rate of 250 kS/s. A simple voltage divider circuit was constructed with a known resistance of 3.3 Ω as one of its components and other being the electrode pair. DAQ device is controlled by custom software written in MATLAB®. A sine wave V_{in} of 1V amplitude was applied across the circuit using one of the channels of DAQ device and output voltages V_{out1} and V_{out2} were recorded across electrode pair and known resistance respectively through separate output channels of DAQ device. Since there is a known resistance in the circuit, current I through it can be measured as $I = V_{out2}/R$. The same current flows through the series circuit and impedance magnitude of the electrode pair can be measured using the same current I as $|Z| = V_{out1}I$. Impedance phase θ was measured by taking phase difference between the voltage across electrode pair V_{out1} and current I through them as $\angle\theta = \angle\theta_V - \angle\theta_I$.

Complex impedance is represented by its real and imaginary components in the Cartesian form is given as $Z = R + X_c$. The real and imaginary parts of impedance can be calculated using $|Z|$ and θ as $R = |Z|cos\theta$ and $X_c = |Z|sin\theta$, respectively.

The bipolar impedance of 8 electrode pairs (E20-E19, E18-E17 and so on) was recorded with this impedance meter at room temperature. For switching between 8 electrode pairs, two 74HC4051 8-to-1 multiplexers were used. Multiplexers were controlled by digital output signals from another DAQ device (6009). Six select lines of two multiplexers were connected to the digital output ports of 6009 DAQ device as shown in Fig. 2 as a block diagram.

The overall setup of the complete system is shown in Fig. 3. The plastic cochlear model glued on a support was placed inside a glass filled with saline. the electrode

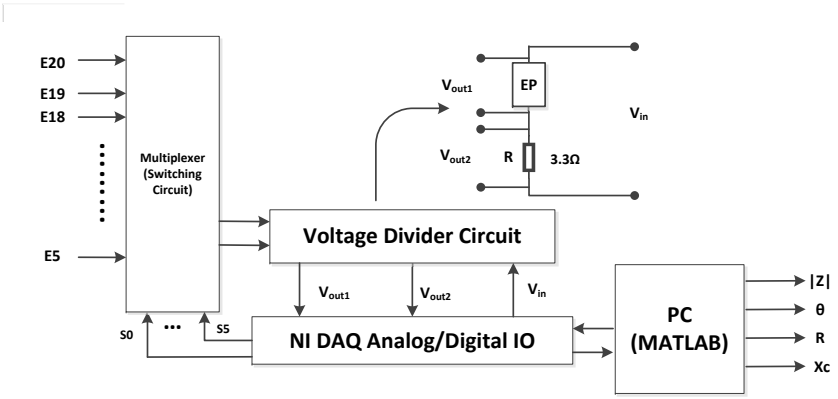

Fig. 2: Impedance Meter and Switching Circuit Setup: 16 Electrodes E20-E5 are connected to multiplexers, 6 select signals S0-S5 are controlling selection of electrode pair for measurement, NI DAQ device is generating and measuring voltages to calculate impedance magnitude, phase, real and imaginary parts.

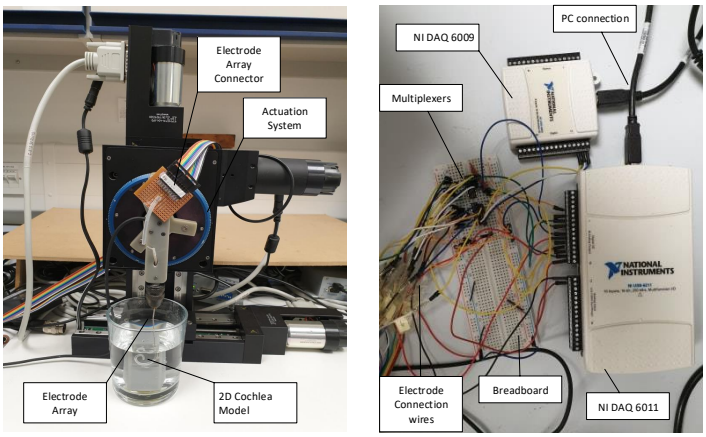

Fig. 3: Experimental Setup (a) Actuation System (b) Impedance meter with the switching circuit connected to electrode wires.

array was placed on a holder attached to the actuation system. Experiments were performed by inserting the electrode array at a speed of 0.05 mm/s for 25 mm depth and bipolar impedance magnitude and phase measurements of each pair were recorded sequentially during the insertion. It took 500 seconds to complete the insertion. The impedance meter samples a pair every 1.5 s, so 41 samples of each electrode pair were taken during the insertion process and analysed offline using Python 3.6.

RESULTS AND DISCUSSION

Bipolar complex impedance of apical 16 electrodes in pairs of 8 were recorded sequentially during the insertion of the electrode array in a plastic ST model. Figure 4 shows four instances during insertion; A) 4 electrodes inserted, B) 8 electrodes inserted, C)16 electrodes inserted, D) 20 electrodes inserted. The arrows show the location of the tip of EA. Figure 5 shows impedance magnitude ($|Z|$), phase (θ), real (R) and imaginary (X_c) parts during insertion. The recordings not only depicts the changes in values when EA is closely placed to the wall (compared to when it is not) but also shows changes when a specific electrode is rubbing (exerted pressure/force) along the wall. It is important to note that when an electrode pair is not in the saline solution (not entered ST model), it gave a high open-circuit impedance value and these values are ignored and not included in the graphs.

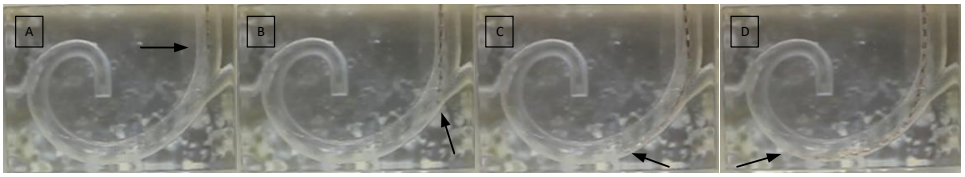

Fig. 4: Electrode array insertion in 2D scala tympani plastic model.

Comparing Fig.4 and Fig.5, EP1 (E19-E20) and EP2 (E17-E18) were inside the model

and away from the wall at instance A. At instance B, E20 (most apical electrode) was starting to touch the lateral wall for the first time and all measurements of EP1 (E19-E20) were starting to change. $|Z|$ from 2.5 kΩ to 3.2 kΩ, θ is getting less negative from -36° to -33°, impedance real part (resistance R) increased from 2 kΩ to 2.7 kΩ, and impedance imaginary part (reactance X_c) from 1.5 kΩ to 1.8 kΩ. In the same way, after 4 samples (between instance B and C) second pair EP2 (E17-E18) came in to contact with the wall and its electrical properties starting to change in the same way. A significant change in measured values were also observed in subsequent electrode pairs EP3(E15-E16), EP4(E13-E14), EP5(E11-E12) just before instance C until instance D, however, there is no significant change in complex impedance of EP6(E9-E10), EP7(E7-E8) and EP8 (E5-E6) as they do not come in to contact with the wall during the insertion process. Figure 6 shows percent change of values during whole insertion (when a particular pair is in saline filled cochlear model) in $|Z|$, θ, R, and X_c of EP1 (apical), EP4 (middle) and EP7 (basal) which clearly shows EP1 has more pronounced change than EP4 due to more contact pressure on it whereas EP7 has no significant change as this pair did not come in to contact with the outer wall.

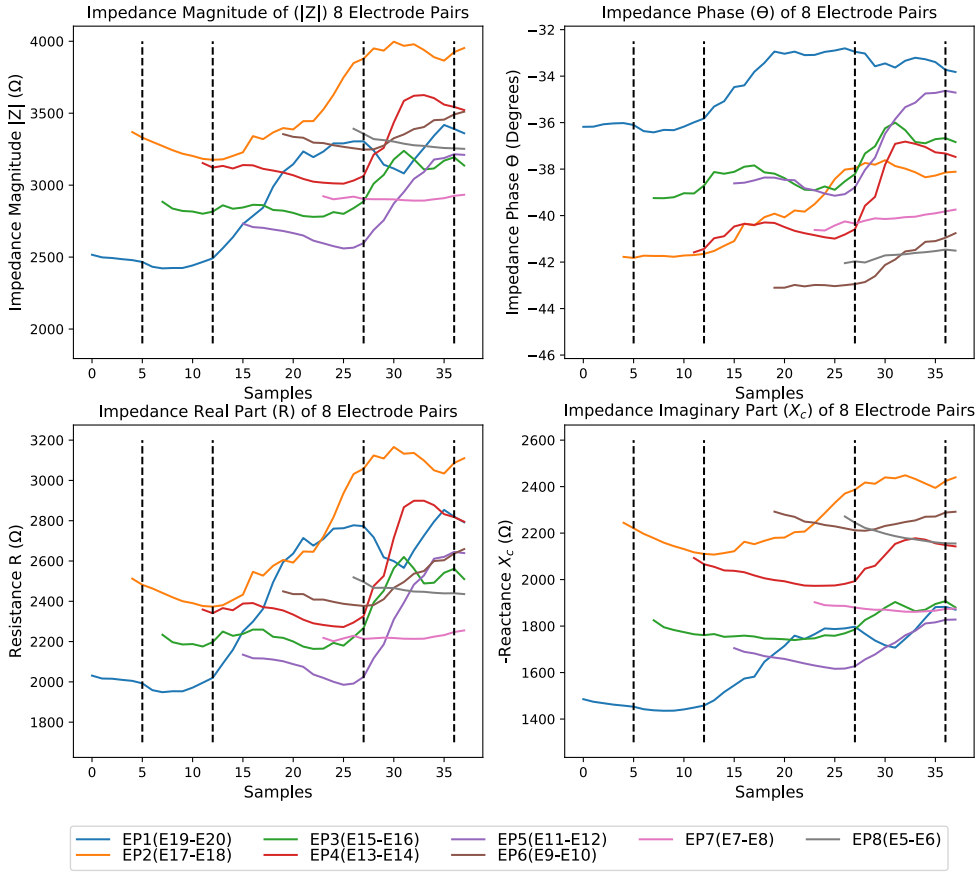

Fig. 5: Impedance magnitude $|Z|$, phase θ, resistance R and capacitive reactance X_c of 8 electrode pairs during insertion.

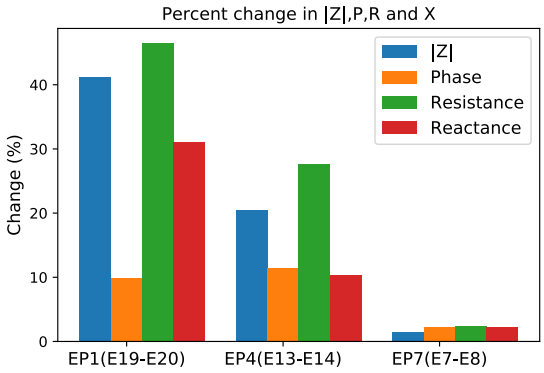

Fig. 6: Percent change (from minimum to maximum values) in impedance magnitude $|Z|$, phase θ, resistance R and capacitive reactance X_c of electrode pair 1, 4 and 7.

We are considering an impedance model of an electrode pair with polarization impedance (resistance and capacitance in parallel) of each electrode contact and an access resistance R_a in series with these polarization impedances $(R1||C1)R_a(R2||C2)$. An increase in $|Z|$ due to wall contact suggested that there is more resistance path between the electrodes. The more negative phase θ implies that impedance is more resistive than capacitive and this phenomenon can also be seen in R and X_c graphs where the change in R is more pronounced than in reactance. Also, an increase in reactance means a decrease in polarization capacitance according to relation $X_c = 1/2\pi fC$.

These results are mainly due to three reasons: 1) disturbance in the chemical reaction at the electrode-electrolyte interface due to wall contact pressure/force, 2) when the array gets closer to the wall, there would be a decrease in reacting electrolyte with electrodes and between electrodes, and 3) impedance of the plastic material is higher than saline.

CONCLUSION

According to current research, there is enough evidence of a relation between EA placement procedure with hearing outcomes and bipolar complex impedance measurements may be used as a sensing technology for localization of EA during cochlear implant surgery. Impedance change due to electrode proximity to different material and application of pressure/force can have application in other electrode implants. These results may be used as feedback control for the actuation system for EA insertion in implantation to manoeuvre it precisely.

REFERENCES

Clark, J.R., Leon, L., Warren, F.M., and Abbott, J.J. (**2012**). "Magnetic guidance of cochlear implants: Proof-of-concept and initial feasibility study," J. Med. Devices, **6**(3). doi: 10.1115/1.4007099.

Dhanasingh, A. and Jolly, C. (**2017**). "An overview of cochlear implant electrode array designs," Hear. Res., **356**, 93–103. doi:10.1016/j.heares.2017.10.005.

Eshraghi, A.A., Nazarian, R., Telischi, F.F., Rajguru, S.M., Truy, E., and Gupta, C. (**2012**). "The cochlear implant: Historical aspects and future prospects," Anat. Rec., **295**, 1967–1980. doi: 10.1002/ar.22580.

Giardina, C.K., Krause, E.S., Koka, K., and Fitzpatrick, D.C. (**2018**). "Impedance measures during in vitro cochlear implantation predict array positioning," IEEE. Trans. Biomed. Eng., **65**, 327–335.

Kontorinis, G., Lenarz, T., Stöver, T., and Paasche, G. (**2011**). "Impact of the insertion speed of cochlear implant electrodes on the insertion forces," Otol. Neurotol., **32**, 565–570. doi: 10.1097/mao.0b013e318219f6ac.

Pile, J., Sweeney, A.D., Kumar, S., Simaan, N., and Wanna, G.B. (**2017**). "Detection of modiolar proximity through bipolar impedance measurements," Laryngoscope, **127**, 1413–1419. doi: 10.1002/lary.26183.

Rau, T.S., Hussong, A., Leinung, M., Lenarz, T., and Majdani, O. (**2010**). "Automated insertion of preformed cochlear implant electrodes: Evaluation of curling behaviour and insertion forces on an artificial cochlear model," Int. J. Comput. Assist. Radiol. Surg., **5**, 173–181.

Rebscher, S.J., Hetherington, A., Bonham, B., Wardrop, P., Whinney, D., and Leake, P.A. (**2008**). "Considerations for the design of future cochlear implant electrode arrays: Electrode array stiffness, size and depth of insertion," J. Rehabil. Res. Dev., **45**, 731.

Richard, C., Fayad, J.N., Doherty, J., and Linthicum Jr, F.H. (**2012**). "Round window versus cochleostomy technique in cochlear implantation: Histological findings," Otol. Neurotol., **33**, 1181. doi: 10.1097/mao.0b013e318263d56d.

Roland, P.S. and Wright, C.G. (**2006**). "Surgical aspects of cochlear implantation: Mechanisms of insertional trauma," In *Cochlear and Brainstem Implants* (Karger Publishers), **64**, 11–30. doi: 10.1159/000094642.

Tan, C.T., Svirsky, M., Anwar, A., Kumar, S., Caessens, B., Carter, P., Treaba, C., and Roland Jr, J.T. (**2013**). "Real-time measurement of electrode impedance during intracochlear electrode insertion," Laryngoscope, **123**, 1028–1032.

Zhang, J., Bhattacharyya, S., and Simaan, N. (**2009**). "Model and parameter identification of friction during robotic insertion of cochlear-implant electrode arrays," Robot. Autom., **2009**, 3859–3864. doi: 10.1109/robot.2009.5152738.

Zhang, J., Wei, W., Ding, J., Roland Jr, J.T., Manolidis, S., and Simaan, N. (**2010**). "Inroads toward robot-assisted cochlear implant surgery using steerable electrode arrays," Otol. Neurotol., **31**, 1199–1206.